

# Stark-induced adiabatic Raman ladder for preparing highly vibrationally excited quantum states of molecular hydrogen

Nandini Mukherjee, William E Perreault and Richard N Zare<sup>1</sup>

Department of Chemistry, Stanford University, Stanford, CA 94305, United States of America

E-mail: [zare@stanford.edu](mailto:zare@stanford.edu)

Received 13 April 2017

Accepted for publication 9 June 2017

Published 26 June 2017



CrossMark

## Abstract

We present a multi-color ladder excitation scheme that exploits Stark-induced adiabatic Raman passage to selectively populate a highly excited vibrational level of a molecule. We suggest that this multi-color coherent ladder excitation provides a practical way of accessing levels near the vibrational dissociation limit as well as the dissociative continuum, which would allow the generation of an entangled pair of fragments with near-zero relative kinetic energy. Specifically, we consider four- and six-photon coherent excitation of molecular hydrogen to high vibrational levels via intermediate vibrational levels, which are pairwise coupled by two-photon resonant interaction. Using a sequence of three partially overlapping, single-mode, nanosecond laser pulses we show that the sixth vibrational level of  $H_2$ , which is too weakly coupled to be easily accessed by direct two-photon Raman excitation from the ground vibrational level, can be efficiently populated without leaving any population stranded in the intermediate level. Furthermore, we show that the fourteenth vibrational level of  $H_2$ , which is the highest vibrational level in the ground electronic state with a binding energy of 22 meV, can be efficiently and selectively populated using a sequence of four pulses. The present technique offers the unique possibility of preparing entangled quantum states of H atoms without resorting to an ultracold system.

Keywords: coherent ladder excitation, adiabatic passage, Stark-induced process, Raman excitation

(Some figures may appear in colour only in the online journal)

## Introduction

Historically, an enormous research effort has been directed toward preparing large densities of highly excited molecules, especially those close to or just beyond the vibrational dissociation limit. Inelastic collision of vibrationally excited  $H_2$  controls the thermodynamics and chemistry of interstellar clouds; therefore, preparation of  $H_2$  molecules in highly vibrationally excited states has important implications in astrophysics and astrochemistry [1] as well as fundamental chemical physics scattering studies. Of particular interest is the preparation of a large number of pairs of entangled atoms

with near-zero relative translational energy. So far, preparation of such exotic quantum states has been limited to ultracold systems [2]. In this paper we present a novel vibrational ladder climbing technique that prepares large densities of highly vibrationally excited quantum states without resorting to ultracold or otherwise trapped molecular systems.

In general, optical preparation of a selected highly vibrationally excited quantum state of a molecular gas at room temperature or in a supersonically expanded molecular beam poses a great challenge. To meet this challenge, various Raman adiabatic passage techniques have been developed in the past [3–5]. This family of techniques relies heavily on the two transition dipole matrix elements that couple the initial

<sup>1</sup> Author to whom any correspondence should be addressed.

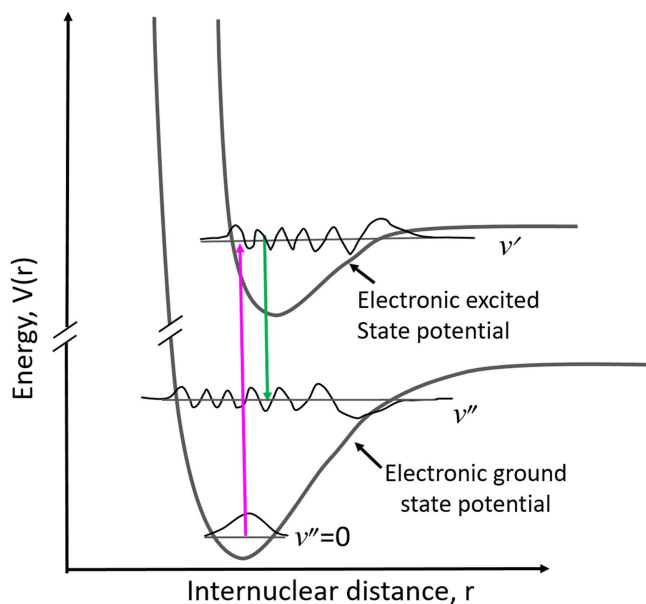


**Figure 1.** Overlap of vibrational wave functions of the ground and excited electronic state involved in an up–down  $\Lambda$  transition.

and the target vibrational levels of the ground electronic state with that of an excited electronic state. These dipole matrix elements should be of sufficient strength to support the adiabatic Raman transition from the initial to the final vibrational state. With increasing vibrational quantum number of the target state, the wave function overlap, that is the Franck–Condon overlap associated with the transition dipole matrix connecting the ground and excited electronic state, becomes weaker (see figure 1), making it problematic to achieve a successful adiabatic Raman passage.

Consider, for example, stimulated Raman adiabatic passage (STIRAP) [3–5], which requires comparable strengths for the Rabi frequencies associated with the pump and Stokes transitions. This requirement clearly cannot be met for arbitrary states high on the vibrational ladder. Increasing light intensity to compensate for weak transition strengths will not work for STIRAP because it relies on the two-photon resonance being strictly maintained; the high intensity light will cause Stark shifts destroying the two-photon resonance condition. One way to compensate for the weaker Rabi frequency is to increase interaction time, such that the adiabaticity of the eigenstates is maintained. This approach makes STIRAP particularly well suited to ultracold molecular systems [6–9].

An alternative technique, which also exploits an intermediate resonance to efficiently populate a highly excited vibrational level is known as Stark-chirped rapid adiabatic passage (SCRAP) [10–12]. To transfer population successfully, SCRAP requires a sufficiently strong Rabi frequency for each leg of the up–down  $\Lambda$  transition, such that the adiabatic following condition is satisfied in the presence of Stark-induced frequency sweeping. Unlike STIRAP, SCRAP populates a real intermediate level in the excited electronic state, so the process is subject to radiative losses. Consequently, SCRAP requires the Rabi frequency to be stronger than the spontaneous emission rate, limiting its application to

fairly strongly coupled vibrational levels. A third member of this family of techniques is Stark-induced adiabatic Raman passage (SARP) [13–16]. SARP is an off-resonant Raman technique that requires the two-photon Rabi frequency to meet a certain threshold value in order to satisfy the condition of adiabatic following as the energy levels are dynamically shifted by the intense optical fields of the partially overlapping laser pulses. The strength of the two-photon Raman coupling relies on the same type of transition dipole matrix element involved in STIRAP and SCRAP. In each of these processes, the adiabatic coupling between the ground and the excited target state generally becomes weaker with increasing wavenumber number of the target vibrational state. This fact makes it very difficult to directly access an arbitrary state high on the vibrational ladder from the ground state of a diatomic molecule.

The efficiency of adiabatic population transfer can be greatly increased by improving the overlap of the vibrational wave functions using ladder excitation where each step up the vibrational ladder is accomplished using an appropriate Raman adiabatic passage. This idea of using multiple coupled Raman adiabatic passages through a set of favorable intermediate vibrational levels to populate a high vibrational state of the ground electronic state has been extensively developed for STIRAP [3, 17–19]. For this procedure, referred to as multistate STIRAP, it was shown that a zero eigenvalue eigenstate can be prepared for the adiabatic Hamiltonian of the multistate system by applying a counterintuitive sequence of pump and Stokes pulses where the Stokes pulses precede the pump pulses. For each transition up the vibrational ladder, multistate STIRAP requires a pair of phase- and frequency-locked pump and Stokes pulses, resonantly tuned to the two-photon transition frequency. This imposes stringent requirements on the laser sources making it difficult or practically impossible to apply to small molecules like hydrogen which require extreme ultraviolet laser sources to resonantly couple states of the ground and excited electronic surfaces. Here we describe a new excitation approach that uses SARP to connect each rung of a multi-step vibrational ladder within the ground electronic state. Because SARP is an off-resonant Raman technique, it can make use of commercially available visible or near visible single-mode pulsed lasers to prepare vibrationally excited quantum states for many small molecules of interest, including hydrogen. This process is capable of efficiently transferring population to any selected high-lying target state of a molecular gas at room temperature or in a beam using a minimal number of single-mode, nanosecond laser pulses.

SARP has been demonstrated to invert population between a pair of vibrational levels within the ground electronic state using a spatially coincident sequence of a pump pulse partially overlapping in time with a Stokes pulse. A detailed description of our prior work developing SARP can be found elsewhere [13–16]. We show here that SARP can be generalized into a continuously coupled, multiphoton adiabatic passage scheme which uses one or more intermediate vibrational states having strong Raman transition dipole matrix elements to access molecular states weakly coupled to the ground state. The present

method, which we call multi-color SARP, not only provides a means to reach a weakly coupled vibrational state using nano-second laser pulses, it has general applicability for preparing high-lying vibrational states of diatomic molecules like  $\text{H}_2$ , HD,  $\text{D}_2$ ,  $\text{N}_2$ , CO, HCl, etc. which have a wide energy gap between the ground and lowest-lying excited electronic states. Moreover, using multi-color SARP, a single or superposition of  $M$  states within a single rovibrational energy eigenstate can be prepared.

In the following sections, we briefly describe the central idea of Stark-induced adiabatic passage, present the theory of multi-color SARP, and discuss the results of our numerical calculations which show that multi-color SARP can achieve complete population transfer to the vibrationally excited  $v = 6$  and  $v = 14$  levels of molecular hydrogen.

### Stark-induced adiabatic following

SARP, by virtue of being an adiabatic passage based technique, relies on following the light-induced dressed states of the molecule in the presence of intense pump and Stokes laser pulses. Adiabatic following requires a threshold value of the two-photon Raman coupling for the successful population transfer to the target state [13, 16]. The adiabatic following condition, also called the Landau–Zener condition [20], can be expressed as

$$d\Delta/dt < 2\pi \Omega^2. \quad (1)$$

Thus, the efficiency of SARP is determined by two key parameters: the Stark sweeping rate, that is, the chirping of the molecular energy levels,  $d\Delta/dt$ ; and the two-photon Rabi frequency,  $\Omega$ . The dynamic Stark shift is determined by the molecular polarizabilities at the laser frequency [13]

$$\Delta = -[\alpha_2(\omega) - \alpha_1(\omega)] |E(\omega)|^2 / \hbar, \quad (2)$$

where  $\alpha_j(\omega)$  is the polarizability of the  $j$ th level at the optical frequency  $\omega$ , and  $E(\omega)$  is the electric field associated with the pump or Stokes laser pulse. For a given Stark sweeping rate, the Landau–Zener condition requires a threshold value for the two-photon Rabi frequency, which is given by  $\Omega = (r_{12}/\hbar)E_P E_S^*$ , where  $E_P$  and  $E_S$  are the electric fields associated with the pump and Stokes laser pulses and  $r_{12}$  is the two-photon Raman coupling coefficient, which is defined by [13, 16, 21]

$$r_{12} = \frac{1}{\hbar} \sum_k \mu_{1k} \mu_{k2} \left[ \frac{1}{\omega_{k1} - \omega_P} + \frac{1}{\omega_{k1} + \omega_S} \right]. \quad (3)$$

Here the subscripts 1 and 2 refer to the initial and final vibrational levels within the ground electronic state of the molecule, respectively. These levels satisfy the two-photon resonant condition with the pump and Stokes photons:  $\omega_{21} = \omega_P - \omega_S$ . The summation index  $k$  represents the vibronic levels belonging to the manifold of excited electronic states. The product of the transition dipole matrix elements  $\mu_{1k} \mu_{k2}$  in equation (3) depends on the overlap of the vibrational wave functions of the ground and excited electronic states. When the product of the overlap integrals becomes too

small,  $r_{12}$  and  $\Omega$  become too weak to satisfy the condition of adiabatic following defined in equation (1).

In the case of molecular hydrogen, Chelkowski and Bandrauk [22] calculated the Raman transition dipole matrix elements for the fundamental and overtone transitions assuming that the molecular axis is aligned with the laser electric field and using 18 intermediate vibrational levels from the  $\text{H}_2$  B  $^1\Sigma_u^+$  state, which is the lowest-lying electronic state of  $\text{H}_2$  that is connected to the ground state by an allowed dipole transition. They found that  $r_{12}$  changes by more than two orders of magnitude with changing target vibrational level, becoming especially small for the ( $v = 0, J = 0$ ) to ( $v = 6, J = 0$ ) overtone transition, namely, about 1/200 of the value for the fundamental Raman transition from ( $v = 0, J = 0$ ) to ( $v = 1, J = 0$ ). For reference, their value of  $r_{12}$  for the ( $v = 0, J = 0$ ) to ( $v = 14, J = 0$ ) overtone transition is approximately 1/40 of the value for the fundamental Raman transition. We have previously shown that both of these Raman couplings are too small for successful SARP [16].

We show here that the limitation imposed by weak vibrational wave function overlap can be overcome using a multi-color SARP ladder which uses a pump pulse partially overlapping with two or more weaker Stokes pulses. Multi-color SARP uses selected, strongly coupled intermediate vibrational levels to increase the overlap of the vibrational wave functions while reducing the Stark sweeping rate of each individual transition between the successive rungs of the vibrational ladder. Here, we specifically develop this method in the case of three-color, four-photon SARP, which allows the preparation of the most weakly coupled Raman level of molecular hydrogen within the ground electronic state, specifically,  $\text{H}_2$  ( $v = 6, J = 0$ ) [22]. Additionally, we show that the multi-color SARP ladder can be generalized to climb the vibrational levels close to the vibrational dissociation of the electronic ground state. Using the specific example of four-color six-photon SARP we calculate that  $\text{H}_2$  ( $v = 14, J = 0$ ), which is the highest level in the vibrational ladder, can be selectively populated with nearly the complete population of the  $\text{H}_2$  ( $v = 0, J = 0$ ) vibrational level.

### Theory of four-photon three-color SARP

To present the central idea of multicolor SARP we develop the Schrödinger equation for a three-level Raman system shown in figure 2, under the action of a pump field  $E_P$  and two Stokes fields  $E_{S1}$  and  $E_{S2}$ . Generalization to four or higher number of intermediate vibrational levels, achieved by increasing the number of overlapping Stokes pulses, is straightforward. For simplicity, we assume the pump and Stokes optical fields to be polarized along the quantization  $z$ -axis:  $\vec{E}_P = \hat{z} E_P \exp(i\omega_P t) + \text{cc}$  and  $\vec{E}_{Sk} = \hat{z} E_{Sk} \exp(i\omega_{Sk} t) + \text{cc}$  with  $k = 1$  and 2 for the two Stokes fields.  $E_P \equiv E_P(t)$  and  $E_{Sk} \equiv E_{Sk}(t)$  represent the slowly varying envelopes of the pump and Stokes laser fields, respectively. Each successive pair of levels in the three-level Raman system is coupled by a two-photon resonant transition. The pump field  $E_P$  and one of the Stokes fields,  $E_{S1}$ , couple the initial state  $|1\rangle$  with the

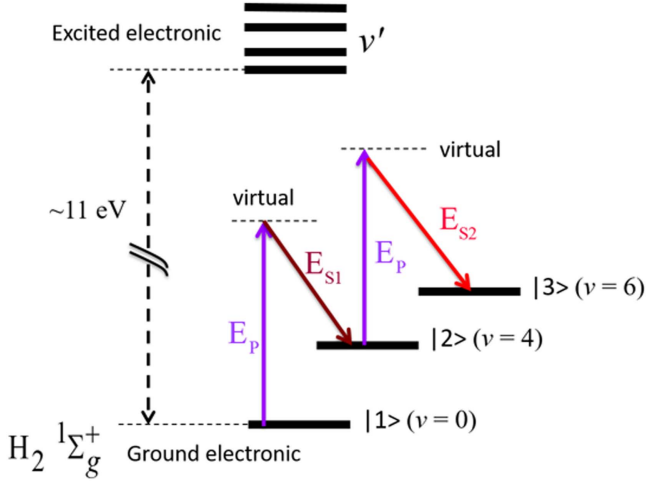


**Figure 2.** Three-level Raman system within the ground electronic state of  $H_2$ . The state vectors  $|1\rangle$ ,  $|2\rangle$ , and  $|3\rangle$  represent the ground  $H_2$  ( $v = 0$ ), and excited  $H_2$  ( $v = 4$ ), and  $H_2$  ( $v = 6$ ) vibrational levels.  $|1\rangle$  and  $|2\rangle$  are coupled by a two-photon resonant Raman transition using the pump and Stokes optical fields  $E_P$  and  $E_{S1}$ . The pump field  $E_P$  and Stokes field  $E_{S2}$  couple  $|2\rangle$  and  $|3\rangle$  by a two-photon resonant interaction. The four-photon interactions of a single pump with two Stokes fields  $E_{S1}$  and  $E_{S2}$  strongly couples the ground state  $|1\rangle$  and the target state  $|3\rangle$ .

intermediate state  $|2\rangle$ , satisfying the two-photon resonant condition  $\omega_P - \omega_{S1} = \omega_{21}$ . Similarly, the intermediate state  $|2\rangle$  is two-photon resonantly coupled to the target state  $|3\rangle$  by the pump field  $E_P$  and the second Stokes field  $E_{S2}$ . The optical fields of the pump and Stokes laser pulses perturb the molecular wave function, which can be expressed as

$$|\Psi(t)\rangle = c_1(t)|1\rangle + c_2(t)|2\rangle + c_3(t)|3\rangle + \sum_{k=1,2,3} c_k(t)|k\rangle, \quad (4)$$

where the  $c$ 's represent the time-dependent amplitudes describing mixing of the molecular bare eigenstates under the influence of the strong electric fields of the lasers.

We follow the approach of Chelkowski and Bandrauk [22] to adiabatically solve for the off-resonant amplitudes  $c_k$  (for  $k \neq 1, 2, 3$ ), and express them in terms of the resonant amplitudes  $c_1$ ,  $c_2$ , and  $c_3$ . In this way we derive the Schrödinger equations for the three-level Raman system. In the rotating wave approximation (RWA), the Schrödinger equation for the three-level Raman system can be expressed as

$$\frac{d}{dt} \begin{pmatrix} c_1 \\ c_2 \\ c_3 \end{pmatrix} = -i \begin{bmatrix} \Delta_{11} & \Omega_{12} & 0 \\ \Omega_{21} & \Delta_{22} & \Omega_{23} \\ 0 & \Omega_{32} & \Delta_{33} \end{bmatrix} \begin{pmatrix} c_1 \\ c_2 \\ c_3 \end{pmatrix}. \quad (5)$$

Here

$$\Delta_{ii} = -[\alpha_i(\omega_P) |E_P|^2 + \alpha_i(\omega_{S1}) |E_{S1}|^2 + \alpha_i(\omega_{S2}) |E_{S2}|^2] / \hbar \quad (6)$$

for  $i = 1, 2$ , and  $3$  are the AC Stark shifts of the field-free eigenstates  $|1\rangle$ ,  $|2\rangle$ , and  $|3\rangle$ .

$\Omega_{12}$  and  $\Omega_{23}$  are the two-photon Rabi frequencies for transitions between  $|1\rangle$  and  $|2\rangle$  and between  $|2\rangle$  and  $|3\rangle$ ,

respectively:

$$\Omega_{12} = \frac{r_{12}}{\hbar} E_P E_{S1}^* e^{i\delta_{12}t}, \quad \Omega_{23} = \frac{r_{23}}{\hbar} E_P E_{S2}^* e^{i\delta_{23}t}. \quad (7)$$

Because we remove the fast oscillating terms using RWA, the Stark shifts  $\Delta_{ii}$  and the two-photon Rabi frequencies  $\Omega_{ij}$  in equations (5)–(7), are expressed in terms of the slowly varying envelopes  $E_P$ ,  $E_{S1}$ , and  $E_{S2}$  of the pump and Stokes optical fields. In equation (7)  $\delta_{12} = \omega_P - \omega_{S1} - \omega_{21}$  and  $\delta_{23} = \omega_P - \omega_{S2} - \omega_{32}$  are the field-free detunings, and  $r_{12}$  and  $r_{23}$  are the couplings for the two-photon Raman transitions, as defined in equation (3), between the pairs of states  $|1\rangle$  and  $|2\rangle$ , and  $|2\rangle$  and  $|3\rangle$ , respectively.

To numerically demonstrate the adiabatic population transfer using multicolor SARP, we consider two specific examples that prepare the ( $v = 6$ ,  $J = 0$ ), and ( $v = 14$ ,  $J = 0$ ) levels of molecular  $H_2$  from the ground ( $v = 0$ ,  $J = 0$ ) level.

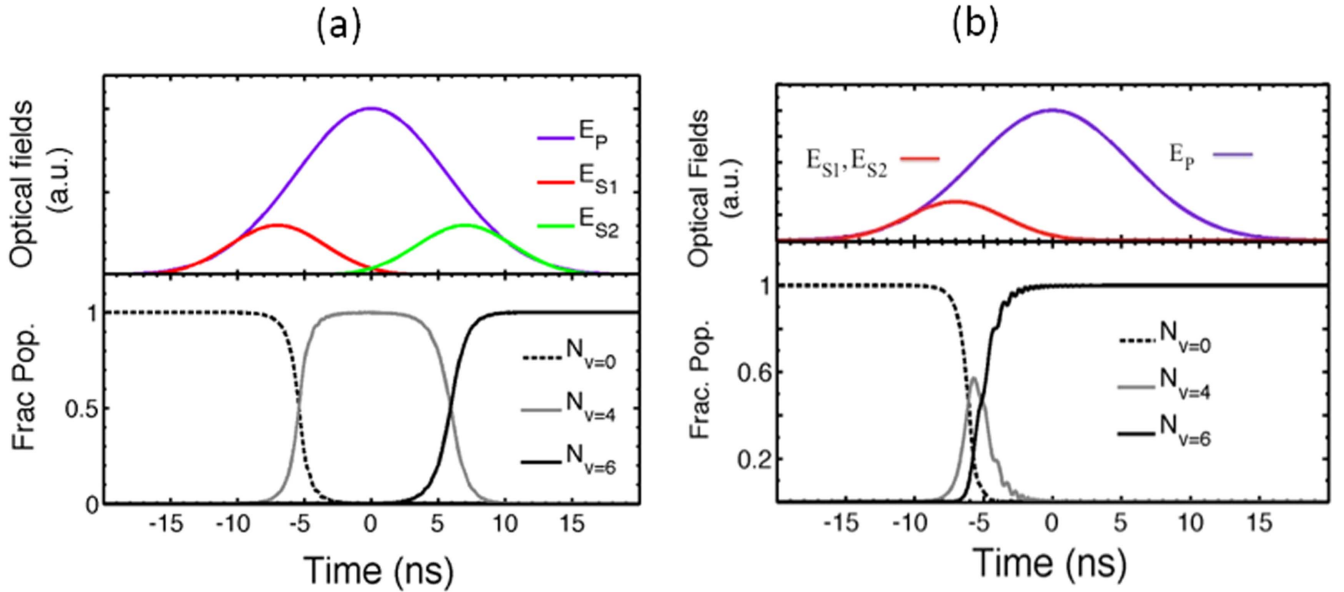
### Vibrational ladder climbing of $H_2$ using three- and four-color SARP

In this section, we first present the results of our numerical calculations to show that using a sequence of a strong pump pulse partially overlapping in time with two weaker Stokes pulses (see figure 3), a three-color SARP ladder can be used to selectively populate the ( $v = 6$ ,  $J = 0$ ) level of  $H_2$  molecule via the intermediate level  $H_2$  ( $v = 4$ ,  $J = 0$ ). Then we extend our calculations to a four-color SARP ladder to reach the highest vibrational level,  $H_2$  ( $v = 14$ ,  $J = 0$ ), below the dissociation limit via two intermediate vibrational levels,  $H_2$  ( $v = 4$ ,  $J = 0$ ) and  $H_2$  ( $v = 9$ ,  $J = 0$ ). We show that using a strong pump pulse partially overlapping in time with three weaker Stokes pulses, the four-color SARP ladder selectively transfers nearly the complete population of  $H_2$  ( $v = 0$ ,  $J = 0$ ) to  $H_2$  ( $v = 14$ ,  $J = 0$ ). In each of these cases, nearly complete population transfer to the target levels is accomplished adiabatically when the strong pump pulse sweeps the Raman transition frequency in the presence of the time-delayed Stokes pulses.

To numerically integrate equation (5), we estimate the polarizabilities and the two-photon Raman coupling coefficients using transition dipole matrix elements that are derived from the vibrationally resolved transition probability data for  $B^1\Sigma_u^+ \rightarrow X^1\Sigma_g^+$ ,  $C^1\Pi_u \rightarrow X^1\Sigma_g^+$ , and  $B'^1\Sigma_u^+ \rightarrow X^1\Sigma_g^+$  transitions involving 40 vibronic states [23]. The  $M$ -state dependencies of the dynamic Stark shifts,  $\Delta_{ii}$ , and the two-photon Rabi frequencies,  $\Omega_{ij}$ , are evaluated for the linearly polarized pump and Stokes optical fields along the quantization  $z$  axis for the various pairs of two-photon coupled levels involved in the multi-color SARP ladder. Table 1 summarizes the pulse parameters, the peak AC Stark shifts, and the peak Rabi frequencies for the relevant transitions considered in the following applications of three and four-color SARP. For numerical integration, we consider Gaussian temporal profiles of the form  $\exp[-(t/\tau)^2]$  for the optical fields representing the pump and Stokes pulses.

**Table 1.** Wavelength, fluence, and temporal length of the Gaussian pump and Stokes pulses used in the calculation. Also listed are the peak AC Stark shifts and the peak Rabi frequencies for the coupled Raman transitions involved in the three and four-color ladder SARP.

Transition	Pump $E_P$	Stokes $E_{S1}$	Stokes $E_{S2}$	Stokes $E_{S3}$	Peak Stark shift (GHz)	Peak Rabi frequency (GHz)
$\nu = 0 \rightarrow \nu = 4$	355 nm	773 nm	456 nm	—	$\Delta_{40} = -10$	$\Omega_{04} = 0.5$
$\nu = 4 \rightarrow \nu = 6$	$12 \text{ J mm}^{-2}$	$1 \text{ J mm}^{-2}$	$1 \text{ J mm}^{-2}$		$\Delta_{64} = -7$	$\Omega_{46} = 0.8$
	$\tau = 8 \text{ ns}$	$\tau = 5 \text{ ns}$	$\tau = 5 \text{ ns}$			
$\nu = 0 \rightarrow \nu = 4$	355 nm	773 nm	710 nm	523 nm	$\Delta_{40} = -10$	$\Omega_{04} = 0.5$
$\nu = 4 \rightarrow \nu = 9$	$12 \text{ J mm}^{-2}$	$1 \text{ J mm}^{-2}$	$1 \text{ J mm}^{-2}$	$1 \text{ J mm}^{-2}$	$\Delta_{94} = -16$	$\Omega_{49} = 0.57$
$\nu = 9 \rightarrow \nu = 14$	$\tau = 8 \text{ ns}$	$\tau = 5 \text{ ns}$	$\tau = 5 \text{ ns}$	$\tau = 5 \text{ ns}$	$\Delta_{149} = 10.6$	$\Omega_{149} = 0.35$

**Figure 3.** Fractional population in  $\nu = 0, 4,$  and  $6$  levels as function of time during the three-color SARP process. Population transfer is accomplished with a strong pump pulse  $E_P$  partially overlapping with two weaker Stokes pulses  $E_{S1}$  and  $E_{S2}$ . The pump pulse has a fluence of  $12 \text{ J mm}^{-2}$  and a Gaussian temporal profile with duration of  $8 \text{ ns}$ . Each Stokes pulse is also of Gaussian shape with duration of  $5 \text{ ns}$ , having a fluence of  $1 \text{ J mm}^{-2}$ . The upper panel of each plot shows the pulse sequence as a function of time while the lower panel shows the fractional population in  $\nu = 0$  ( $N_{\nu=0}$ , dash black),  $\nu = 4$  ( $N_{\nu=4}$ , solid gray) and  $\nu = 6$  ( $N_{\nu=6}$ , solid black). In (a), the first Stokes pulse  $E_{S1}$  is applied  $7 \text{ ns}$  earlier and the second Stokes  $E_{S2}$  is applied  $7 \text{ ns}$  later than the pump pulse (sequential SARP). In (b), both Stokes pulses are applied simultaneously,  $7 \text{ ns}$  earlier than the pump pulse (ladder SARP).

### Preparation of $\text{H}_2$ ( $\nu = 6, J = 0$ ) using three-color SARP

Figure 3 shows the temporal dynamics of two different pulse configurations of three-color four-photon SARP that prepares the ( $\nu = 6, J = 0$ ) level. In figure 3(a) the population is carried from the initial to the target level via the intermediate ( $\nu = 4, J = 0$ ) level using two consecutive SARP processes. As the Stark shift of the  $\nu = 0$  to  $\nu = 4$  Raman transition is swept by the rising intensity of the pump pulse, the first SARP adiabatically carries the population from  $\nu = 0$  to  $\nu = 4$  in the presence of a delayed Stokes pulse  $E_{S1}$ . The  $\nu = 0$  to  $\nu = 4$  transition is red shifted by  $10 \text{ GHz}$ , and a field-free Stokes detuning  $\delta_{04} = 5.5 \text{ GHz}$  is used to achieve the complete population transfer. The second SARP then takes the population from  $\nu = 4$  to the target  $\nu = 6$  level as the Raman frequency for the  $\nu = 4 \rightarrow 6$  transition is swept by the falling intensity of the pump in the presence of the

second Stokes pulse  $E_{S2}$ . This transition is also red shifted and a field-free Stokes detuning  $\delta_{46} = 4 \text{ GHz}$  is used to accomplish complete population transfer to the target  $\text{H}_2$  ( $\nu = 6, J = 0$ ) level. We call this ‘sequential SARP.’ Clearly this scheme goes in two separate steps, as opposed to the one shown in figure 3(b) where the two Stokes pulses are applied simultaneously,  $7 \text{ ns}$  earlier relative to the pump pulse. In this case, a coupled or ladder-like excitation occurs without ever fully populating the intermediate ( $\nu = 4$ ) state. We call this ‘ladder SARP’. In both cases, at the end of the three-pulse cycle nearly all population is transferred to the target  $\text{H}_2$  ( $\nu = 6, J = 0$ ) level without leaving population in the intermediate  $\nu = 4$  level. In the following sections, we show that the continuous adiabaticity of ladder SARP allows it to reach a very high vibrational state or even to adiabatically dissociate a molecule.

The sequential and ladder SARP described above resemble the D-SCRAP and T-SCRAP processes [12] developed

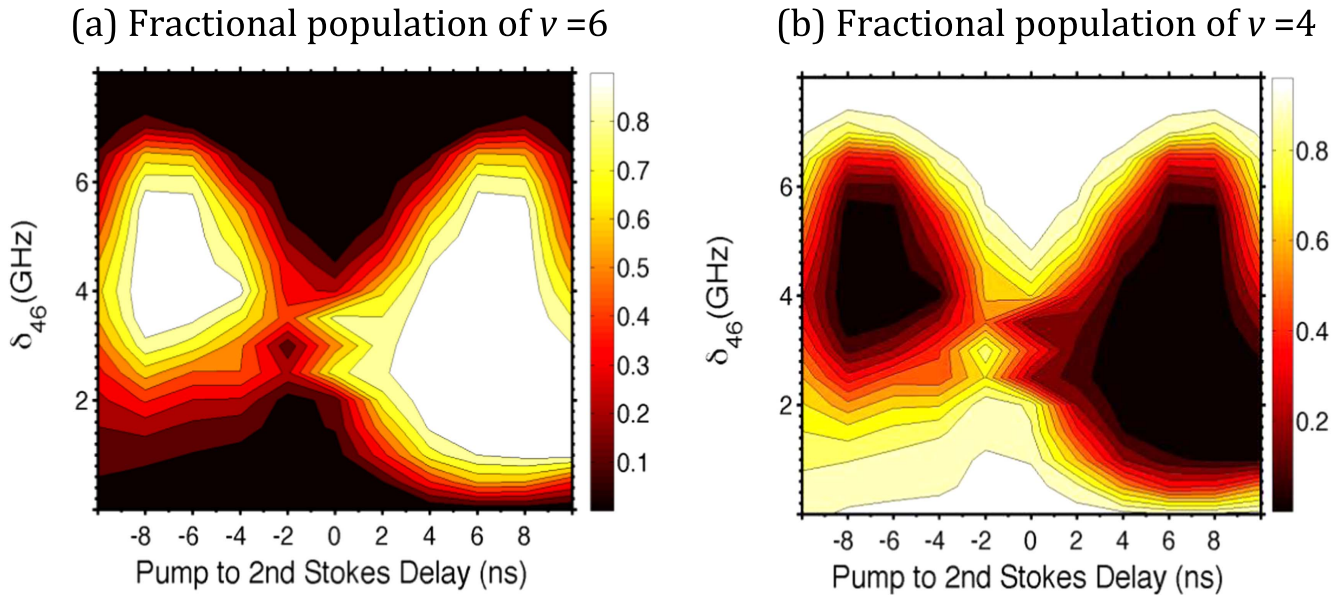


**Figure 4.** Contour plot of the fractional population in the (a)  $\nu = 6$  and (b)  $\nu = 4$  levels at the end of the pulse sequence of three-color SARP plotted as a function of the field-free detuning  $\delta_{46}$  and delay of the 2nd Stokes field  $E_{S2}$  relative to the pump field  $E_p$ . The delay and frequency detuning of the first Stokes pulse is held fixed. The first Stokes  $E_{S1}$  is applied 7 ns earlier than the pump pulse. The field-free detuning  $\delta_{04}$  of the first Stokes pulse for the  $0 \rightarrow 4$  Raman transition is kept fixed at 5.5 GHz corresponding to the complete population transfer in figure 3. The white area in (a) represents greater than 95% population transfer to  $\nu = 6$ . The complementary plot in (b) shows that for the same range of delay and frequency detuning almost no population is stranded in intermediate level  $\nu = 4$  during the adiabatic Raman passage. The fluence of the pump and Stokes pulses are the same as in figure 3.

earlier for the selective excitation of a vibrational level. Although all of these techniques are Stark-induced adiabatic passage processes, we again note an important difference between these methods. D-SCRAP and T-SCRAP are three-photon processes that accomplish population transfer between a pair of vibrational levels of the ground electronic state via a resonant intermediate excited electronic state. Because the intermediate state in the three-photon  $\Lambda$  transition is an electronically excited state, the problem of vibrational, or Franck–Condon, overlap as described in the introduction persists for target states high on the vibrational ladder. Moreover, because these processes utilize a radiatively coupled real intermediate state, they are vulnerable to both radiative and ionization losses. Furthermore, for small molecules like  $H_2$ , D-SCRAP and T-SCRAP will require single-mode vacuum ultraviolet laser sources which are not only difficult to obtain but also will cause significant ionization losses from the near resonant intermediate state. Multi-color SARP, on the hand, is an adiabatic ladder climbing that takes the population through the nonradiatively coupled vibrational levels of the electronic ground state. This gives multi-color SARP the ability to enhance the vibrational overlap of a weak direct transition by connecting it through small steps in the vibrational ladder. Because SARP is not limited by radiative losses, weaker Rabi frequencies can always be compensated using longer pulses. Additionally, SARP does not need to resonantly connect to an excited electronic state, making it much easier to apply to hydrogen and other small molecules which have large energy gaps between the ground and excited electronic states.

Figure 4 shows a contour plot of the fractional population in  $\nu = 6$  (figure 4(a)), and  $\nu = 4$  (figure 4(b)), as a function

of the delay and detuning of the second Stokes field  $E_{S2}$ . Figure 4(a) exhibits both sequential and ladder SARP, showing that both have significant bandwidths over which complete population of the initial ( $\nu = 0, J = 0$ ) level can be transferred to the ( $\nu = 6, J = 0$ ) level. As the delay is changed from sequential SARP to ladder SARP there is quite obviously a region wherein there is little to no population of the target state, which is caused by coherent population return [24]. Figure 4(b) shows that for both sequential and ladder SARP, no population is stranded in the intermediate ( $\nu = 4, J = 0$ ) level over a significant bandwidth.

### Preparation of a pair of loosely bound H-atoms using four-color ladder SARP

Using a sequence of three overlapping Stokes pulses with a partially overlapping stronger pump pulse, we carried out calculations of multi-color ladder SARP exciting  $H_2$  from ( $\nu = 0$ ) to ( $\nu = 14$ ), the highest vibrational level within the ground electronic state. The ( $\nu = 14$ ) level is 22 meV or  $177 \text{ cm}^{-1}$  below the vibrational dissociation limit of  $H_2$  [23, 25]. We use ( $\nu = 4$ ) and ( $\nu = 9$ ) as the intermediate levels. For this system, the  $3 \times 3$  Hamiltonian in equation (5) is generalized to a  $4 \times 4$  Hamiltonian describing interaction with the four Raman coupled vibrational levels ( $\nu = 0, 4, 9,$  and  $14$ ) in the ladder transition. Figure 5 describes the temporal dynamics of the adiabatic population transfer via the intermediate vibrational levels.

The top panel of figure 5 shows the three overlapping Stokes pulses of equal intensity placed on the left wing of a

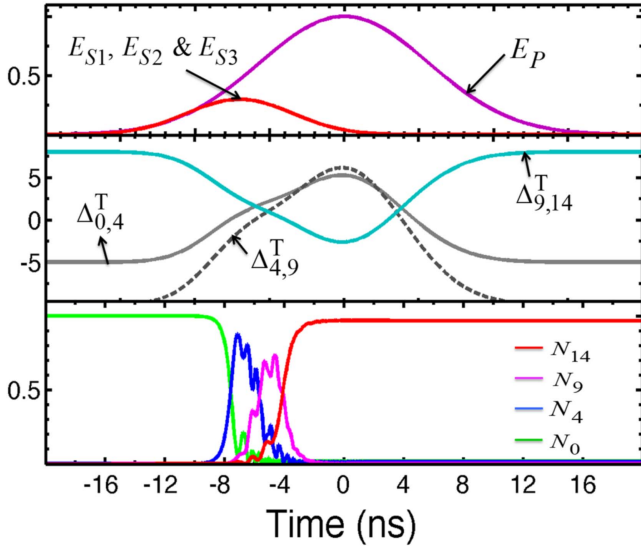


**Figure 5.** Temporal dynamics of a four-color ladder SARP preparing  $\text{H}_2$  ( $v = 14$ ,  $J = 0$ ) via the intermediate  $\text{H}_2$  ( $v = 4$ ,  $J = 0$ ) and  $\text{H}_2$  ( $v = 9$ ,  $J = 0$ ). The three Stokes pulses are combined on the left wing of a stronger pump pulse with a delay of 7 ns as shown in the upper panel of the figure. The middle panel shows the dynamic detuning (GHz) of the three different Raman transitions associated with the three steps of the vibrational ladder. The lower panel shows the dynamics of adiabatic population flow through the various vibrational levels of the ladder.

stronger pump pulse. The fluences and durations for the pump and Stokes pulses are listed in table 1. The Stokes pulses appear 7 ns earlier than the pump pulse. The middle panel shows the net dynamic detuning in GHz associated with each Raman transition connecting the rungs of the vibrational ladder. The net dynamic detuning for the transition ( $v = i$ ) to ( $v = j$ ) is defined as  $\Delta_{ij}^T = \delta_{ij} - (\Delta_{ij} - \Delta_{ii})$ , where  $\delta_{ij}$  is the field free detuning and  $(\Delta_{ij} - \Delta_{ii})$  is the net AC Stark shift as defined in equations (5)–(7). Note that the Stark-induced detuning for the ( $v = 9$ )  $\rightarrow$  ( $v = 14$ ) transition has the opposite sign relative to the other two intermediate Raman transitions. The bottom panel shows the fractional population in the four vibrational levels ( $v = 0$ , 4, 9, and 14) as a function of the pulse time. It is readily seen that population transfer takes place as each transition is Stark-shifted into resonance in turn. At the end of the excitation, essentially no population is stranded in either of the intermediate levels.

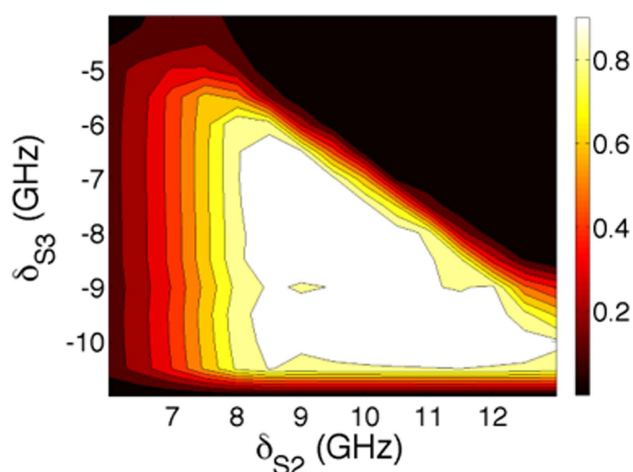
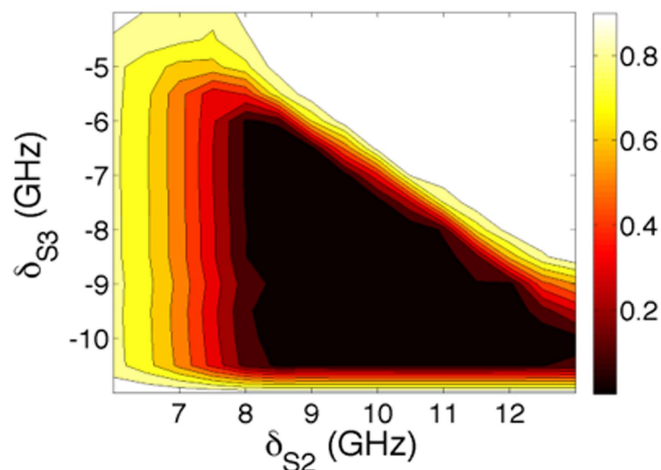
Figure 6(a) shows a contour plot of the population transfer to  $\text{H}_2$  ( $v = 14$ ) as a function of the second Stokes detuning  $\delta_{S2}$  (for  $v = 4 \rightarrow v = 9$  transition), and the third Stokes detuning  $\delta_{S3}$  (for  $v = 9 \rightarrow v = 14$  transition), while the detuning for the first Stokes is held at a constant value of  $\delta_{S1} = 5$  GHz corresponding to the peak of the  $\text{H}_2$  ( $v = 0$ ) to  $\text{H}_2$  ( $v = 4$ ) transition. The contour plot shown in figure 6(b) confirms that no population is stranded in the two intermediate vibrational levels ( $v = 4$ ) and ( $v = 9$ ). The bandwidth shown in these plots demonstrates that nearly complete population transfer to the highest vibrational level is feasible using commercially available, single-mode, nanosecond laser sources. Additionally, we have performed calculations on sequential four-color SARP, where Stokes pulses  $S_1$  and  $S_2$

are placed on the rising wing of the pump pulse and the third Stokes pulse  $S_3$  is placed on the falling wing of the pump. In this case, we see a much larger bandwidth over which the entire population is transferred to ( $v = 14$ ), further demonstrating the practicality of this technique.

## Discussion

We have shown that multi-color SARP, operating in sequential or ladder-like fashion, is able to completely transfer population to a single, specific highly vibrationally excited state. Particularly noteworthy is ladder SARP's ability to climb in a continuously adiabatic manner, leaving no population stranded in intermediate states. Thus, it can make use of a large number of intermediate states without compromising the selectivity or the transfer efficiency for preparing a desirable target state. It is this fact that allows it to overcome the problem of small Rabi frequencies discussed in the introduction by improving the vibrational overlap. Multi-color SARP gains an additional advantage compared to the direct transition by reducing the relative dynamic Stark shift between each pair of two-photon coupled levels. Further, being an off-resonant Raman process, it completely avoids any radiatively coupled excited electronic states. This is advantageous both in that it is not restricted by the excited state lifetime and in that it does not require detailed knowledge of the excited state potential surface.

At this point a comparison of the multi-color SARP presented here with the four-photon STIRAP used to create a degenerate quantum gas of ground state molecules of  $\text{Cs}_2$  starting from magnetically associated loosely bound Feshbach molecules [19] is in order. In the specific example of  $\text{Cs}_2$ , the exceptionally long coherence time available in the ultracold regime played an essential role by allowing the very long interaction time required to fulfill the adiabaticity for weak transitions. In the photoassociation of  $\text{Cs}_2$ , the transfer efficiency was limited to 50%–60% by the linewidth and or the intensity of the lasers coupling the intermediate single-photon transitions. For STIRAP to function, it is necessary that the two-photon resonance, or dark state condition, between the pair of levels  $|1\rangle$  and  $|3\rangle$  and  $|3\rangle$  and  $|5\rangle$  of the five-level system always be maintained. As we have pointed out in the introduction, because of the necessity of maintaining these resonances over the period of optical interaction, the transfer efficiency is heavily reliant on two key factors. First, the transition dipole matrix elements, or the Franck–Condon overlap, between the ground and excited electronic surfaces must be sufficiently strong such that the corresponding Rabi frequencies are much larger than the inverse coherence time. Second, to maintain coherence for sufficiently long interaction time, it requires multiple narrow linewidth phase-locked lasers, which must be also frequency-locked to individual single-photon resonances, making it a technologically challenging system, particularly for small molecules like  $\text{H}_2$  which require extreme ultraviolet laser sources for resonant Raman excitation. In addition, it should be noted that achieving the ultracold temperatures necessary for long

(a) Fractional population of  $\nu = 14$ (b) Fractional population of  $\nu = 4 + \nu = 9$ 

**Figure 6.** (a) Contour plot of the population transferred to  $\nu = 14$  as a function of the second Stokes detuning  $\delta_{S2}$  (for  $\nu = 4 \rightarrow \nu = 9$  transition), and the third Stokes detuning  $\delta_{S3}$  (for  $\nu = 9 \rightarrow \nu = 14$  transition), while the detuning for the first Stokes is held at a constant value of  $\delta_{S1} = 5$  GHz corresponding to the peak of the  $H_2$  ( $\nu = 0$ ) to  $H_2$  ( $\nu = 4$ ) transition. The pulse sequence is the same as in figure 5. (b) Contour plot of the total intermediate state population ( $N_4 + N_9$ ) as a function of the second and third Stokes detunings,  $\delta_{S2}$  and  $\delta_{S3}$ .

coherence times remains an unsolved challenge in molecular hydrogen, as well as many other small molecules of interest.

Alternatively, the multi-color SARP presented here provides a robust approach to reach a weakly coupled target level high in the vibrational ladder for a low-pressure molecular gas at room temperature or in a molecular beam using a single-mode nanosecond pump pulse partially overlapping in time with multiple Stokes laser pulses. Because multicolor SARP does not require a strict two-photon resonance condition between the successive steps of the vibrational ladder, laser intensity can be increased to better fulfill the adiabaticity for relatively weakly coupled transitions. In addition, multi-color ladder SARP improves wave function overlap by increasing the number of intermediate steps, as we have shown in the preparation of the ( $\nu = 14$ ) level of the  $H_2$  molecule. Stretching the molecule far from equilibrium opens possibilities in probing long range interactions which become more important at low temperatures. Additionally, the weakening of bonds using high vibrational excitation enables the study of reactive collisions at low translational temperatures which would be otherwise forbidden in the ground vibrational state. Multi-color SARP can also be applied to polyatomic molecules, opening many more possibilities for interesting studies of collisional dynamics far from equilibrium.

We note that a multi-color SARP ladder can prepare a high rotational level with selected  $M$  states, thus preparing a highly aligned molecular ensemble, which has potential applications in studying stereochemistry. We suggest that the Raman ladder excitation process shown here could be applied to enhance coupling cross sections to dissociative states which have minimal vibrational overlap with the ground state. In this way, we believe that multi-color SARP's ability to operate in a ladder-like fashion could provide a unique way to achieve coherent dissociation, creating pairs of entangled atoms with high density.

## Acknowledgments

This work has been supported by the US Army Research Office under ARO Grant No. W911NF-16-1-1061, and MURI Grant No. W911NF-12-1-0476.

## References

- [1] Agundez M, Goicoechea J R, Cernicharo J, Faure A and Roueff E 2010 *Astrophys. J.* **713** 662
- [2] Gneiting C and Hornberger K 2008 *Phys. Rev. Lett.* **101** 260503
- [3] Vitinov N V, Fleischhauer M, Shore B W and Bergmann K 2001 *Adv. At., Mol., Opt. Phys.* **46** 55
- [4] Vitinov N V, Halfmann T, Shore B W and Bergmann K 2001 *Annu. Rev. Phys. Chem.* **52** 763
- [5] Bergmann K, Vitinov N V and Shore B W 2015 *J. Chem. Phys.* **142** 170901
- [6] Koch C P and Shapiro M 2012 *Chem. Rev.* **112** 4928
- [7] Ospelkaus S, Pe'er A, Ni K-K, Zirbel J J, Neyenhuis B, Kotochigova S, Julienne P S, Ye J and Jin D S 2008 *Nat. Phys.* **4** 622
- [8] Winkler K, Lang F, Thalhammer G, Straten P V D, Grimm R and Denschlag H 2007 *Phys. Rev. Lett.* **98** 043201
- [9] Danzl J G, Haller E, Gustavsson M, Mark M J, Hart R, Bouloufa N, Dulieu O, Ritsch H and Nägerl H-C 2008 *Science* **321** 1062
- [10] Rangelov A A, Vitinov N V, Yatsenko L P, Shore B W, Halfmann T and Bergmann K 2005 *Phys. Rev. A* **72** 053403
- [11] Oberst M, Münch H and Halfmann T 2007 *Phys. Rev. Lett.* **99** 173001
- [12] Oberst M, Münch H, Grigoryan G and Halfmann T 2008 *Phys. Rev. A* **78** 033409
- [13] Mukherjee N and Zare R N 2011 *J. Chem. Phys.* **135** 024201
- [14] Mukherjee N, Dong W, Harrison J A and Zare R N 2013 *J. Chem. Phys.* **138** 051101
- [15] Dong W, Mukherjee N and Zare R N 2013 *J. Chem. Phys.* **139** 074204



- [16] Perreault W E, Mukherjee N and Zare R N 2016 *J. Chem. Phys.* **145** 154203
- [17] Vitanov N V 1998 *Phys. Rev. A* **58** 2295
- [18] Vitanov N V, Shore B W and Bergmann K 1998 *Eur. Phys. J. D* **4** 15
- [19] Danzl J G, Mark M J, Haller E, Gustavsson M, Hart R, Aldegunde J, Hutson J M and Nägerl H-C 2010 *Nat. Phys.* **6** 265
- [20] Rubbmark J R, Kash M M, Littman M G and Kleppner D 1981 *Phys. Rev. A* **23** 3107
- [21] Marcuse D 1980 *Principles of Quantum Electronics* (New York: Academic)
- [22] Chelkowski S and Bandrauk A D 1997 *J. Raman Spectrosc.* **28** 459
- [23] Fantz U and Wunderlich D 2006 *At. Data Nucl. Data Tables* **92** 853
- [24] Mukherjee N and Zare R N 2011 *J. Chem. Phys.* **135** 184202
- [25] Herzberg G 1950 *Spectra of Diatomic Molecules* (New York: Van Nostrand-Reinhold)